The preparation of cobalt phosphide and cobalt chalcogenide (CoX, X = S, Se) nanoparticles from single source precursors†

Weerakanya Maneeprakorn, Mohammad A. Malik and Paul O'Brien*

Received 3rd November 2009, Accepted 18th January 2010
First published as an Advance Article on the web 4th February 2010
DOI: 10.1039/b922804g

Dialkyldiselenophosphinatocobalt(II), $[Co(Se_2PR_2)_2]$ (R = ^{i}Pr, Ph and ^{t}Bu), complexes were used to grow cobalt selenide and cobalt phosphide nanoparticles by decomposition in trioctylphosphine oxide (TOPO) or hexadecylamine (HDA) at 300 °C. Orthorhombic $CoSe_2$ nanoparticles are readily formed in HDA or TOPO, whereas, in TOP/TOPO or TOP/HDA only orthorhombic CoP or Co_2P nanoparticles were formed. This observation suggests that TOP provides the phosphorus for nanoparticles. The composition of cobalt phosphide can be controlled by the reaction time. Co_2P was obtained after 60 min of thermolysis at 300 °C whereas CoP was grown over 150 min. In order to confirm the effect of TOP on the thermolysis of the precursor, the related sulfur containing precursor, $[Co(S_2P^tBu_2)_2]$, was decomposed in TOP/TOPO, TOP/HDA, TOPO or HDA. The thermolysis reaction in TOPO or HDA gave cubic Co_9S_8 nanoparticles whereas in TOP/TOPO or TOP/HDA only CoP nanoparticles were formed as expected due to the presence of TOP. Characterization of these nanoparticles by transmission electron microscopy, X-ray diffraction, and electron diffraction shows highly crystalline spherical CoP and Co_2P nanoparticles with a size of 5 nm diameter, and $CoSe_2$ nanoparticles are close to cubes of *ca.* 10 nm size. Co_9S_8 nanoparticles are aggregates composed of numerous small cuboid Co_9S_8 nanoparticles with average diameters of 10–20 nm. The optical spectra show that Co_2P and CoP nanoparticles have a band gaps (E_g) = 3.14 and 1.71 eV, respectively, whilst $CoSe_2$ nanoparticles a band gap of 1.45 eV.

Introduction

Transition-metal phosphides have a wide range of interesting chemical and physical properties. Metal-rich phosphides (M/P > 1) and monophosphides (M/P = 1) are usually hard, brittle substances with relatively high thermal and electrical conductivities and thermal stability. Transition-metal phosphides are applied as protective refractory coatings in electric lamps, as oxygen barrier layers in capacitors, and in coatings that are resistant to wear and corrosion.[1] Moreover, they also have been extensively investigated as potential components for magnetic application and as superior catalysts.[2] Amongst these, cobalt phosphides have rarely been investigated. The Co–P phase diagram shows both orthorhombic Co_2P and CoP phases. Besides these two phases, the JCPDS database shows three other phases rich in phosphorus: monoclinic CoP_2, cubic CoP_3, and cubic CoP_4.

Cobalt phosphides have been prepared by several methods: Co_2P was prepared by the direct reaction of a phosphine (*e.g.*, PH_3) or phosphorus pentachloride with metallic cobalt or cobalt salts,[3] or by metal-organic chemical vapour deposition[4] or by self-propagating high temperature synthesis routes.[5] However, this approach requires either high reaction temperature (1000 °C) or long annealing periods to obtain highly crystalline materials.[6] Recently, solution-phase synthesis,[7,8] sol–gel methods,[9,10] solid-state method,[11] and solvothermal method,[6,12,13] have also been reported. For example, the nanocluster of Co_2P confined in a silica xerogel matrix was prepared using sol–gel chemistry from single source precursor, $[Co_4(CO)_{10}(\mu\text{-dppa})]$ (dppa = $(Ph_2P)_2NH$).[9] The plate-like orthorhombic Co_2P particles of about 50 nm diameter, with a wide size distribution were prepared by a direct solvothermal reaction of metal halide with yellow phosphorus at mild temperatures (80–140 °C) with ethylenediamine as a solvent.[14] O'Brien *et al.* reported the preparation of the single-crystalline CoP nanowires by thermal decomposition of $Co(acac)_2$ and tetradecylphosphonic acid (TDPA) in a mixture of trioctylphosphine oxide (TOPO) and HDA at 340 °C.[15] Similarly, cubic Co_2P nanorods were synthesized from the thermal decomposition of continuously delivered Co–TOP complex, prepared from reaction of $Co(acac)_2$ (acac = acetylacetone) and trioctylphosphine (TOP) in a mixture of octyl ether (OE) and hexadecylamine (HDA) at 300 °C.[16]

Transition-metal chalcogenides MX (M = Fe, Co, or Ni; X = S or Se) have also attracted attention due to their remarkable properties and potential for application.[17] As an important pyrite-type compound, $CoSe_2$ is known as a metallic conductor and exchange-enhanced Pauli paramagnet in its ground state with a Curie temperature, T_c, of 124 K.[18] However, $CoSe_2$ has rarely been researched as nanoscale materials due to the limited availability of high-quality materials. Usually, the crystalline

The School of Chemistry and Materials Science Center, The University of Manchester, Oxford Road, Manchester, UK M13 9PL. E-mail: paul.obrien@manchester.ac.uk; Fax: + 44 (0)161 275 4598; Tel: +44 (0)161 275 4653

† Electronic supplementary information (ESI) available: XRD patterns of cobalt phosphide nanoparticles obtained from $[Co(Se_2P^tBu_2)_2]$ precursor in TOP/HDA at 300 °C for different reaction times. See DOI: 10.1039/b922804g

$CoSe_2$ has been prepared by solid-state reactions,[19] solvothermal,[17,20] and hydrothermal methods.[21] For example, orthorhombic and cubic $CoSe_2$ were prepared by ball milling of a binary mixture between Co and Se element for milling time up to 30 h.[19] The feather-like orthorhombic $CoSe_2$ nanoparticles with an average diameter of 20 nm were prepared from solvothermal method of $CoCl_2$ and Se powder at 160 °C.[20] The orthorhombic $CoSe_2$ nanorods with diameter of about 70 nm and length up to 1450 nm were prepared in the temperature range 90–170 °C through hydrothermal method.[21]

There are many phases of cobalt sulfides, such as CoS, Co_3S_4, CoS_2, and Co_9S_8. Among them, Co_9S_8 has attracted attention.[22] It is of importance as a hydrodesulfurization catalyst and shows interesting metallic and paramagnetic properties.[23] Cobalt sulfides have often been prepared using solid-state reactions at high temperature (500–1200 °C) but these conditions can lead to a larger particle size and inhomogeneity, and it is difficult to obtain single phase of cobalt sulfide.[24,25] Other methods including the reaction of cobalt or cobalt monoxide with hydrogen sulfide,[26] the treatment of anhydrous cobalt sulfate salt in a stream of H_2S/H_2,[23] as well as hydrothermal method[27,28] have been reported. However, the conditions for obtaining Co_9S_8 are not very specific.

The use of single-source molecular precursors (SSPs), which have both metal source and phosphorus/selenium source in the same structure, has been extensively studied for the growth of metal chalcogenide thin films.[4,29–31] There are only few reports of a SSP for cobalt phosphide nanoparticles.[9,32] However, to the best of our knowledge, the uses of SSP to synthesize cobalt selenide nanoparticles have not been achieved. Co_3Se_4 films with a small component of $CoSe_2$ were prepared by thermolysis of $[Co\{^tBu_2P(Se)N^iPr\}_2]$ and $[Co\{^tBu_2P(Se)NiC_6H_{11}\}_2]$.[33] Recently, we have reported the deposition of cubic Co_9Se_8 and orthorhombic CoP thin films from the single-source precursor $[Co(Se_2P^iPr_2)_2]$ in aerosol-assisted metal-organic chemical vapour deposition (AA-MOCVD).[4] We also reported the preparation of nickel phosphide and nickel selenide nanoparticles from $[Ni(Se_2PR_2)_2]$ (R = ^{i}Pr, ^{t}Bu, and Ph) by thermolysis in TOPO or HDA.[34]

Herein we report one pot synthesis of $CoSe_2$, CoP or Co_2P nanoparticles from $[Co(Se_2PR_2)_2]$ (R = ^{i}Pr, ^{t}Bu, and Ph) and Co_9S_8 from $[Co(S_2P^tBu_2)_2]$, as the SSP into hot coordinated solvent, HDA, TOPO, TOPO/TOP or HDA/TOP. The CoP and Co_2P were obtained using the same precursor just by controlling the growth time.

Experimental

Preparation of precursors

(a) $[Co(Se_2PR_2)_2]$, (R = ^{i}Pr, ^{t}Bu, and Ph). The synthesis of $[Co(Se_2P^iPr_2)_2]$ (**1**), $[Co(Se_2P^tBu_2)_2]$ (**2**), and $[Co(Se_2PPh_2)_2]$ (**3**) was carried out by the method described in the literature.[4,35] This method involved the deprotonation of the ligand $(HNEt_3)(R_2PSe_2)$, where R = ^{i}Pr, ^{t}Bu, and Ph to form the anion which is then reacted with Co(II) chloride hexahydrate in methanol to produce a dialkyldiselenophosphinato cobalt(II) complex.

(b) $[Co(S_2P^tBu_2)_2]$. Solution of $CoCl_2 \cdot 6H_2O$ (2.5 g, 10 mmol) in 25 ml of water was added drop wise to a solution of diisobutyldithiophosphinic acid, $^tBu_2PS_2Na$ (4.6 g, 20 mmol), in 100 ml of methanol and 50 ml of water. The mixture was then stirred for 10 min at room temperature under atmospheric pressure forming green precipitate, which was filtered, washed with methanol and re-crystallized in toluene to obtained green crystals of $[Co(S_2P^tBu_2)_2]$.

Preparation of cobalt phosphide nanoparticles

The method used was essentially the same as that described by Trindade and O'Brien.[36] In a typical reaction, Co_2P nanoparticles were prepared by degassing HDA (10 g) under reduced pressure at 120 °C for 1 h and then heated to 300 °C under nitrogen. $[Co(Se_2P^tBu_2)_2]$ (**2**) precursor (0.5 g) was dissolved in TOP (10 ml) and quickly injected into HDA. The reaction temperature dropped to approximately 290 °C. The reaction mixture was heated again to 300 °C and kept at this temperature for 60 min. The colour of the solution changed from an initial transparent violet to turbid dark brown. The dark solution formed was cooled to approximately 70 °C. An excess of hot methanol was added to the solution to give a black precipitate, which was separated by centrifugation and dried under vacuum. The black precipitate could easily be redispersed in organic solvents, such as chloroform, toluene, hexane, *etc.*

CoP nanoparticles were prepared similarly but increasing the reaction time to 150 min. Similar reactions were carried out in TOPO/TOP system. Attempted reactions at 200 and 250 °C to prepare cobalt phosphide nanoparticles were unsuccessful.

Preparation of cobalt selenide nanoparticles

Cobalt selenide nanoparticles were prepared by thermolysis in TOPO or HDA without TOP. In a typical reaction, $CoSe_2$ nanoparticles were prepared by adding $[Co(Se_2P^iPr_2)_2]$ precursor (0.5 g) in solid HDA (10 g) and then degassing the reaction mixture under reduced pressure at 120 °C for 1 h. The reaction mixture was heated to 320 °C under N_2 and kept at this temperature for 120 min. After 120 min, the dark solution formed was cooled to approximately 70 °C. An excess of hot methanol was added to the solution to give a black precipitate, which was separated by centrifugation and dried under vacuum. The black precipitate could easily be redispersed in organic solvents, such as chloroform, toluene, hexane, *etc.* Other reactions were carried out using TOPO as the capping agent.

Preparation of cobalt sulfide nanoparticles

Cobalt sulfide nanoparticles were prepared by thermolysis $[Co(S_2P^tBu_2)_2]$ precursor in TOPO or HDA without TOP. Co_9S_8 nanoparticles were prepared by adding $[Co(S_2P^tBu_2)_2]$ precursor (0.5 g) in solid HDA or TOPO (10 g) and then degassing the reaction mixture under reduced pressure at 120 °C for 1 h. At this stage, the reaction mixture was melted to violet-blue solution. This solution was then heated to 300 °C under N_2 and kept at this temperature for 45 min. After that, the dark-violet solution formed was cooled to approximately 70 °C. An excess of methanol (or hot methanol in the case of HDA) was added to the solution to give a dark-violet precipitate, which was separated by

centrifugation and dried under vacuum. The dark-violet precipitate could easily be redispersed in organic solvents, such as chloroform or toluene.

Other reactions were carried out using TOPO/TOP and HDA/TOP as the capping agent. Briefly, $[Co(S_2P^tBu_2)_2]$ (0.5 g) was dissolved in TOP (10 ml) and quickly injected into HDA at 300 °C. The reaction temperature dropped to approximately 290 °C. The reaction mixture was heated again to 300 °C and kept at this temperature for 45 min. The colour of the solution changed from an initial transparent violet to dark-violet. The dark-violet solution formed was cooled to approximately 70 °C. First, an excess of hot methanol was added to the solution to give a black gel, which was separated by centrifugation. Then, 50 ml of acetone was added to the black gel to give the black precipitates which was separated and dried under vacuum. The black precipitate could easily be redispersed in organic solvents, such as chloroform and toluene.

Characterization of nanoparticles

The X-ray power diffraction experiments were performed using a Bruker D8 AXE diffractometer (Cu Kα). UV-Vis spectra were measured using a Heλios-Beta Thermospectronic spectrophotometer. The samples were placed in quartz cuvettes (1 cm path length) and the optical measurements were carried out using toluene as a reference. High-resolution transmission electron microscopy (HRTEM) was performed using Tecnai F30 FEG TEM instrument, operating at 300 kV. TEM samples were prepared by evaporating a drop of the material suspended in toluene onto a copper grid covered with carbon film.

Results and discussion

Cobalt phosphide nanoparticles were synthesized by the thermal decomposition of $[Co(Se_2PR_2)_2]$ precursors, R = ^{i}Pr, ^{t}Bu, and Ph, in a hot surfactant solutions of TOPO/TOP or HDA/TOP. Reaction temperature is a key factor in the formation of the cobalt phosphide nanoparticles. No cobalt phosphide nanoparticles were formed at temperatures lower than 300 °C. No precipitate formed with addition of methanol after 1 h of reaction. Moreover, alkyl groups in the precursors have no effect to the chemical composition of the nanoparticles. All precursors, $[Co(Se_2P^iPr_2)_2]$ (**1**), $[Co(Se_2P^tBu_2)_2]$ (**2**), $[Co(Se_2PPh_2)_2]$ (**3**), give only cobalt phosphide instead of cobalt selenide in thermolysis. However, from our previous study of $[Ni(Se_2PR_2)_2]$ precursors, (R = ^{i}Pr, ^{t}Bu, and Ph), which can result in the deposition of either nickel selenide (NiSe, Ni_3Se_2) or nickel phosphides (Ni_2P, $Ni_{12}P_5$, Ni_5P_4) depending upon the nature of the ligand and the conditions.[34] In that work, the coordinating solvents play an important role in the chemical composition of nanoparticles. Nickel phosphide was produced in TOPO/TOP system for all precursors at all reaction temperatures except $[Ni(Se_2P^tBu_2)_2]$ precursor which produced nickel selenide at 280 °C. Whereas, nickel selenide can be obtained in HDA/TOP system from $[Ni(Se_2P^tBu_2)_2]$ and $[Ni(Se_2P^iPr_2)_2]$ precursor at all temperature except $[Ni(Se_2P^iPr_2)_2]$ which produced nickel phosphide.

Fig. 1 shows the XRD patterns of cobalt phosphide nanoparticles obtained from $[Co(Se_2P^tBu_2)_2]$ (**2**) precursor in TOP/TOPO at 300 °C at various growth times. As seen in Fig. 1,

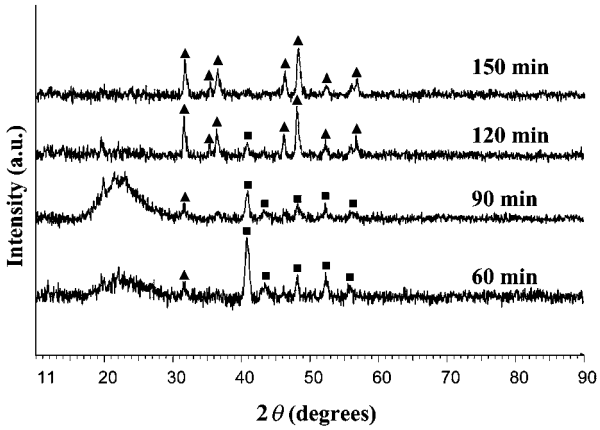

Fig. 1 XRD patterns of cobalt phosphide nanoparticles obtained from $[Co(Se_2P^tBu_2)_2]$ precursor in TOP/TOPO at 300 °C for different reaction time; ■ orthorhombic Co_2P (JCPDS-32-0306), ▲ orthorhombic CoP (JCPDS-29-0497).

growth time is the most important factor determining the formation of crystal phases in the reaction. At 60 min, orthorhombic Co_2P (JCPDS card no. 32-0306) was obtained. Moreover, the broad peak in the region $2\theta \cong 17$–$29°$ and a peak at $2\theta = 31.5°$ corresponding to CoP which appear as contaminant were observed. When the reaction time increased to 90 min, the intensity of that broad peak increased and unidentified peak at $2\theta = 20°$ was observed. At 120 min, the mixture of Co_2P and CoP was obtained and broad peak disappeared. At 150 min, only a pure orthorhombic CoP (JCPDS card no. 29-0497) phase was formed. Increasing the reaction time led to the transformation of Co_2P to CoP.

Similar experiments in TOP/HDA also show the change from Co_2P to CoP phase as the reaction time increased. XRD patterns of cobalt phosphide nanoparticles obtained from $[Co(Se_2P^tBu_2)_2]$ precursor in TOP/HDA at 300 °C for different reaction times were shown in Fig. S1 in ESI†. At 60 min, only orthorhombic Co_2P (JCPDS no: 32-0306) was obtained. When the reaction time increased to 90 min, the unidentified peaks of the reaction intermediate at $2\theta = 20°$, 22° and 29° and the mixture of Co_2P and CoP were obtained. Highly crystalline CoP was finally obtained in 150 min. It is interesting to note that CoP phase started to form in 60 min in TOP/TOPO and in 90 min in TOP/HDA. Our previous studies on using $[Co(Se_2P^iPr_2)_2]$ (**1**) precursor for the deposition of cobalt phosphide or selenide thin films by AA-MOCVD showed that the films deposited at 400 °C are a mixture of cubic Co_9Se_8 and orthorhombic CoP. No deposition was obtained at lower temperature.[4] This shows that at high temperature $[Co(Se_2P^iPr_2)_2]$ precursor can provide both Se and P which can compete to form Co_9Se_8 and CoP. Whereas, in this work, TOP not only acts as the coordinating solvent but also the additional P source which enable the formation of CoP to occur at lower temperature (300 °C). It may also be possible that TOP is simply catalyzing the decomposition of E_2PR_2 ligand to release P atom. Herein we obtained only CoP and Co_2P phases at 300 °C. This indicates that cobalt selenide is formed at higher temperatures and cobalt phosphides at lower temperatures. In addition, the high phosphorus availability *via* TOP decomposition can serve as a source of phosphorus for cobalt phosphides formation.[15,37,38]

In order to prove the role of TOP in the reaction, neat HDA or TOPO was used as capping agent under the same reaction conditions. Fig. 2 shows the XRD patterns of cobalt selenide nanoparticles prepared from thermolysis of $[Co(Se_2P^iPr_2)_2]$ (**1**) precursor at 320 °C for 120 min without TOP in the systems. In HDA, orthorhombic $CoSe_2$ nanoparticles (JCPDS card no. 53-0449) were obtained (Fig. 2(a)) whereas in TOPO the mix phases of orthorhombic $CoSe_2$ (JCPDS card no. 53-0449) and cubic $CoSe_2$ nanoparicles (JCPDS card no. 01-089-2002) were formed (Fig. 2(b)). These results clearly confirm that the phosphorus in cobalt phosphide comes from TOP. Moreover, in the absence of TOP, the nanoparticles tended to form aggregates during the reaction especially in TOPO. Possibly, without TOP the protecting ability of TOPO or HDA as capping agent was reduced.[39]

To confirm the effect of TOP on thermolysis of $[Co(X_2PR_2)_2]$ (X = S or Se; R = ^{i}Pr, ^{t}Bu, and Ph) precursors, the di-*t*-butylthiophosphinatocobalt(II), $[Co(S_2P^tBu_2)_2]$ complex was used as the alternative SSP. Other thermolysis reactions were carried out in TOPO, HDA, TOPO/TOP and HDA/TOP. As expected, in neat TOPO or HDA only cubic Co_9S_8 nanoparticles (JCPDS card no. 01-075-2023) were synthesized (Fig. 3(a) and (b)) whereas, in TOPO/TOP or HDA/TOP system, only an amorphous CoP was formed after addition of methanol, which was evident after annealing at 450 °C for 2 h in argon, and transformed the amorphous material into orthorhombic CoP (JCPDS card no. 01-075-2023) (Fig. 4(a) and (b)). TOPO/TOP or HDA/TOP systems seem to be unsuitable coordinating ligand for preparation of cobalt selenide or sulfide nanoparticles from $[Co(X_2PR_2)_2]$ (X = S or Se; R = ^{i}Pr, ^{t}Bu, and Ph) precursors because metal can cause cleavage of P–C bond, resulting in diffusion of phosphorus into the metal and compete with selenium atom to form the metal phosphide instead of metal selenide.[38,40] Thus, in rich phosphorus environment nanocrystalline cobalt phosphides are the preferred phase over cobalt selenide/sulfide. However, for $[Co(S_2P^tBu_2)_2]$ precursor it is possible that amorphous cobalt phosphide was formed instead of nanocrystalline cobalt phosphide. Moreover, for $[Co(Se_2PR_2)_2]$ precursors (R = ^{i}Pr, ^{t}Bu, and Ph) $CoSe_2$ nanoparticles can be formed only at high temperature (320 °C) and the difference in alkyl groups in the precursor molecules does not show any effect to the chemical composition of the nanoparticles.

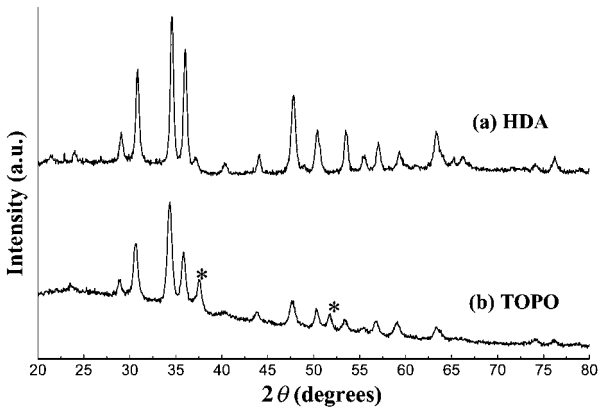

Fig. 2 XRD patterns of orthorhombic $CoSe_2$ nanoparticles (JCPDS card no. 53-0449) prepared from thermolysis of $[Co(Se_2P^iPr_2)_2]$ precursor at 320 °C for 120 min without TOP in (a) HDA and (b) TOPO; * cubic $CoSe_2$ (JCPDS card no. 01-089-2002).

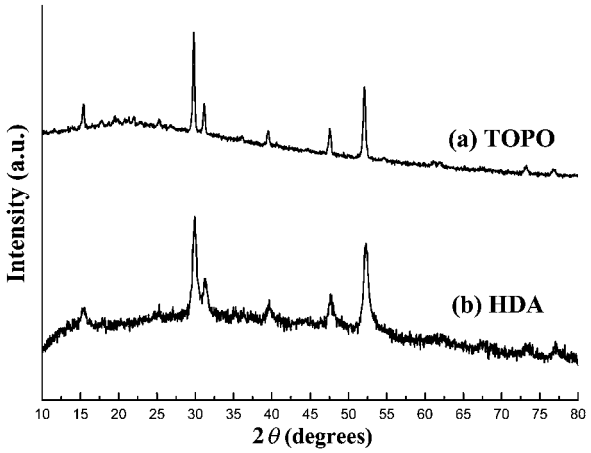

Fig. 3 XRD patterns of the cubic Co_9S_8 nanoparticles prepared from thermolysis of $[Co(S_2P^tBu_2)_2]$ precursor at 300 °C for 45 min in (a) TOPO and (b) HDA (JCPDS card no. 01-075-2023).

The absorption spectra of the Co_2P and CoP nanoparticles appear in the range of 300–800 nm as shown in Fig. 5. The absorption spectrum of Co_2P nanoparticles shows two regions of absorption (Fig. 5(a)). The first band, an intense triplet band at 540, 580 and 625 nm, corresponds to the $^4A_2 \rightarrow {}^4T_1$ (P) transition of high-spin tetrahedral Co^{2+} (d^7) in the cobalt complex which is formed from decomposition of precursor during the reaction.[41,42] Inset in Fig. 5(a) shows the absorption spectrum of $[Co(Se_2P^tBu_2)_2]$ precursor which also shows triplet band of spin-allowed absorption transition of the $^4A_2 \rightarrow {}^4T_1$ (P) transition. This result coincides with the result from XRD which shows an unidentified broad peak at $2\theta \cong 17$–$29°$ at 60 min (Fig. 1.). This can be assigned to the un-decomposed cobalt complex. However, the second excitonic peak at the absorption band edge ≈ 410 nm (3.02 eV) is clearly assigned to a direct band transition of Co_2P nanoparticles. Fig. 5(b) shows the absorption spectrum of CoP.

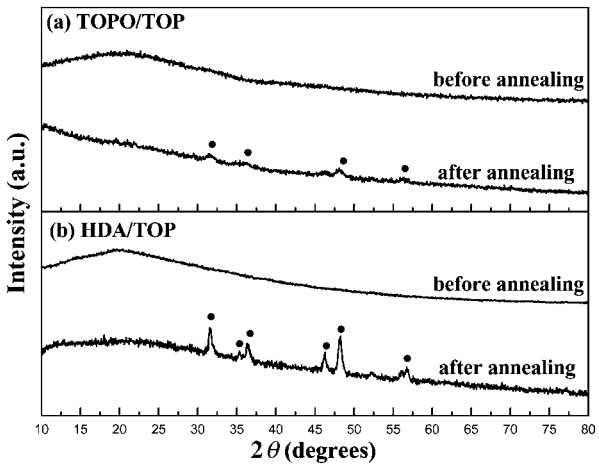

Fig. 4 XRD patterns of the as-prepared samples and the samples after annealing at 450 °C for 2 h in argon. All samples prepared from thermolysis of $[Co(S_2P^tBu_2)_2]$ precursor at 300 °C for 150 min in (a) TOPO/TOP and (b) HDA/TOP; ● orthorhombic CoP (JCPDS card no. 01-075-2023).

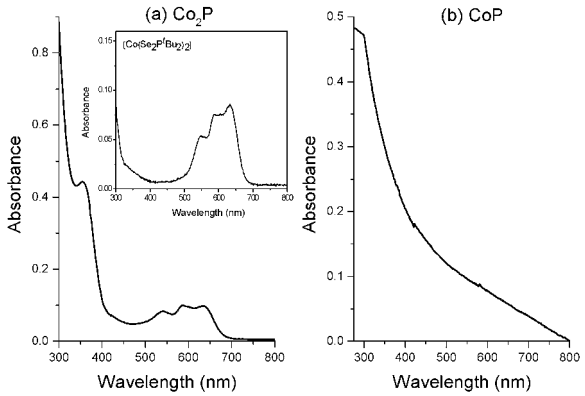

Fig. 5 UV-visible absorption graphs showing the absorbance *vs.* the wavelength for (a) Co_2P obtained from $[Co(Se_2P^tBu_2)_2]$ precursor in TOP/TOPO at 300 °C for 60 min and (b) CoP nanoparticles obtained from $[Co(Se_2P^tBu_2)_2]$ precursor in TOP/TOPO at 300 °C for 150 min; inset shows the absorption graph of $[Co(Se_2P^tBu_2)_2]$ precursor.

The absorption spectrum shows absorption maximum at about 305 nm and exhibits shoulders at about 350 nm. Moreover, a broad tail extends out from about 500 up to 800 nm. The UV-visible absorption spectrum of $CoSe_2$ nanoparticles obtained from $[Co(Se_2P^iPr_2)_2]$ precursor in HDA at 320 °C for 120 min is shown in Fig. 6. The absorption spectrum appears to show three step transitions at absorption edges ≈ 600 nm (2.06 eV), others at ≈ 800 nm (1.55 eV) and ≈ 900 nm (1.38 eV).

There are no reports in the literature for the band gap of $CoSe_2$, Co_2P and CoP. The band gap reported for single crystal of CoP_3 is 0.45 eV.[43] There are the reports for the band gaps of the mixed phases of cobalt phosphides which range from 0.666–0.885 eV.[36] In a crystalline or polycrystalline material both direct or indirect optical transitions are possible depending on the band structure of the material. Assuming parabolic bands, the relation between α and E_g for a direct transition is given by:[44,45]

$$\alpha h\nu = A(h\nu - E_g)^n, \quad (1)$$

and for indirect transition by:[45]

$$\alpha h\nu = \frac{A(h\nu - E_g + E_p)^n}{\exp(\theta_D/T) - 1} + \frac{B(h\nu - E_g - E_p)^n}{1 - \exp(-\theta_D/T)}, \quad (2)$$

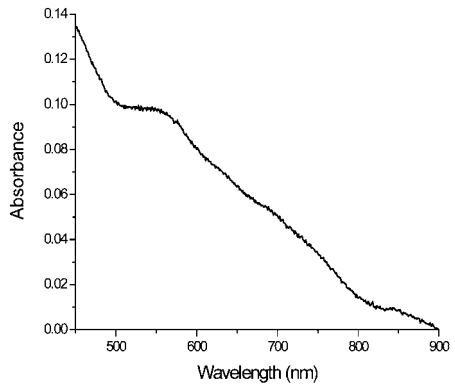

Fig. 6 UV-visible absorption spectrum of $CoSe_2$ nanoparticles obtained from $[Co(Se_2P^iPr_2)_2]$ precursor in HDA at 320 °C for 120 min.

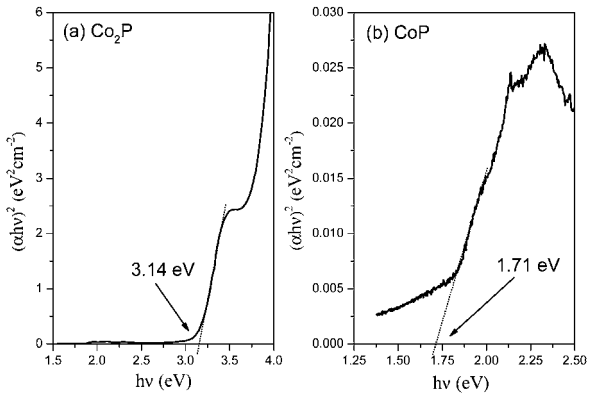

Fig. 7 Graphs showing $(\alpha h\nu)^2$ *vs.* $h\nu$ plot (direct) of (a) Co_2P and (b) CoP nanoparticles for determination of E_g.

where E_p is the phonon energy assisting the transition, θ_D is the Debye temperature and A and B are constants. For a direct transition $n = 1/2$ or 3/2 depending on the nature of the transition. Similarly, $n = 2$ or 3 for indirect transition. The usual method of determining band gap is to plot a graph between $(\alpha h\nu)^{1/n}$ and $h\nu$ and look for that value of n which gives best linear graph in the band edge region. Fig. 7(a) shows the plot between $(\alpha h\nu)^2$ and $h\nu$ of Co_2P nanoparticles. In this case, a linear graph was obtained by using $n = 1/2$. Thus, the Co_2P nanoparticles obtained from this work is direct band gap phosphide which has the band gap (E_g) = 3.14 eV. This value is larger than the values reported elsewhere.[43,44] However, this discrepancy is not unexpected; the band gap of a material also depends on the method of preparation. In case of CoP, the best fit was also obtained for $n = 1/2$ indicating direct transition with band gap (E_g) = 1.71 eV as shown in Fig. 7(b). Fig. 8 shows the plot between $(\alpha h\nu)^2$ and $h\nu$ of $CoSe_2$ nanoparticles. The linear fitting in the region 1.4 eV–2.4 eV corresponds to the sharp edges between 500 nm and 900 nm of absorption spectrum in Fig. 6. The energy band gap (E_g) obtained from extrapolating the linear fitting is 1.45 eV.

Typical TEM images of cobalt phosphide nanoparticles are shown in Fig. 9 and 10. Nanoparticles with a spherical shape are commonly observed for both Co_2P and CoP. Fig. 9 shows the TEM images of orthorhombic Co_2P nanoparticles obtained at 300 °C in TOP/HDA for 60 min. The results from TEM images showed that Co_2P nanoparticles were obtained with an average diameter *ca.* 5 nm (Fig. 9(a)). The ring patterns of selected area

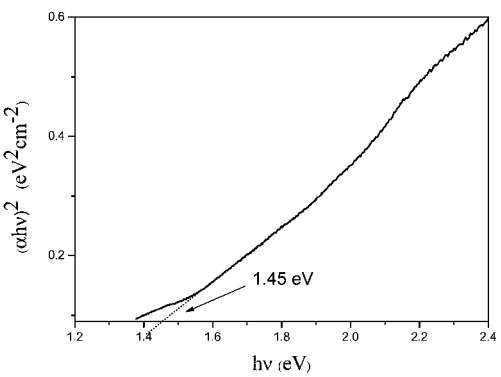

Fig. 8 A graph showing $(\alpha h\nu)^2$ *vs.* $h\nu$ plot (direct) of $CoSe_2$ nanoparticles for determination of E_g.

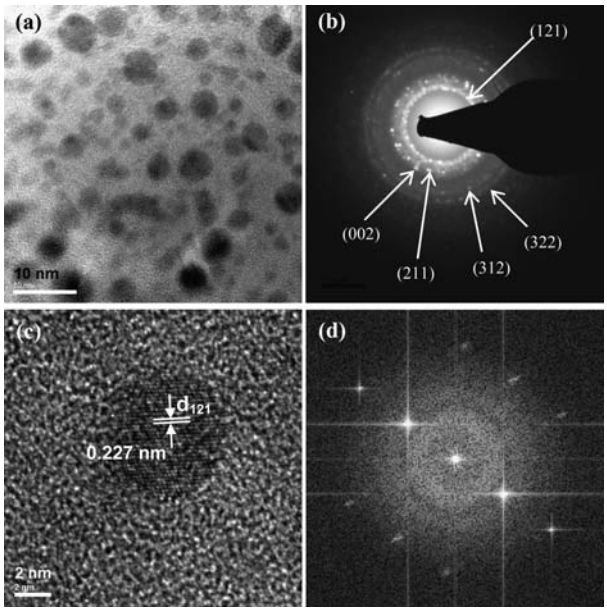

Fig. 9 (a) TEM image of orthorhombic Co_2P nanoparticles, (b) selected area electron diffraction (SAED) pattern, (c) HRTEM image, and (d) FFT of the HRTEM image; all images obtained from $[Co(Se_2P^tBu_2)_2]$ precursor in TOP/HDA at 300 °C for 60 min.

electron diffraction (SAED) (Fig. 9(b)) recorded from Fig. 9(a) are consistent with the (121), (211), (002), (312), and (322) planes of the orthorhombic Co_2P structure. The regularity of the lattice plane in the HRTEM image (Fig. 9(c)) clearly indicates that the Co_2P nanoparticles are single crystals. The space between adjacent planes is 0.227 nm corresponding to the (121) plane. Fast Fourier transform (FFT) diffraction recorded from an individual Co_2P nanoparticle reveals that each nanoparticle is a single crystal (Fig. 9(d)). The morphology of the CoP nanoparticles obtained at 300 °C in TOP/HDA for 150 min is shown in Fig. 10. TEM image of the sample shows that orthorhombic CoP nanoparticles are presented as spherical nanocrystals with the diameter of around 6 nm (Fig. 10(a)). The obvious diffraction rings in the SAED pattern (Fig. 10(b)) recorded from the CoP nanoparticles in Fig. 10(a) can be identified as the (011), (111), (211), and (301) planes of orthorhombic CoP structure. HRTEM image (Fig. 10(c)) clearly showed the lattice fringes with a *d*-spacing of 0.189 nm which corresponds to the (211) plane. Fig. 10(d) shows the FFT of the particles observed in Fig. 10(c) indicated the single-crystalline feature of that particle.

The TEM and HRTEM images of crystalline $CoSe_2$ nanoparticles are shown in Fig. 11. The cuboid $CoSe_2$ nanoparticles with an average length *ca.* 10–20 nm were obtained. The regularity of the lattice plane in the HRTEM image (Fig. 11(b) and (c)) clearly indicates that the $CoSe_2$ nanoparticles are single crystals. The space between adjacent planes is 0.262 nm corresponding to the (111) plane of orthorhombic $CoSe_2$. Fast Fourier transform (FFT) diffraction recorded from an individual Co_2P nanoparticle reveals that each nanoparticle is a single crystal (Fig. 11(d)).

Fig. 12 shows the TEM and HRTEM images of Co_9S_8 nanoparticle prepared from $[Co(S_2P^tBu_2)_2]$ precursor in HDA. Without TOP added, the nanoparticles tended to form the aggregates. As seen in Fig. 12 Co_9S_8 nanoparticles are aggregates composed of numerous small cuboid of Co_9S_8 nanoparticles with an average length *ca.* 15–20 nm (Fig. 12(a) and (b)). Fig. 12(c) shows HRTEM images of cuboid particles which have the space between adjacent planes is 0.298 nm corresponding to the (311) plane of cubic Co_9S_8. In this work, TOP exhibits the important roles not only as phosphorus source for cobalt phosphide nanoparticles but also as the assistant compound to improve the protecting ability of TOPO or HDA as capping agent.

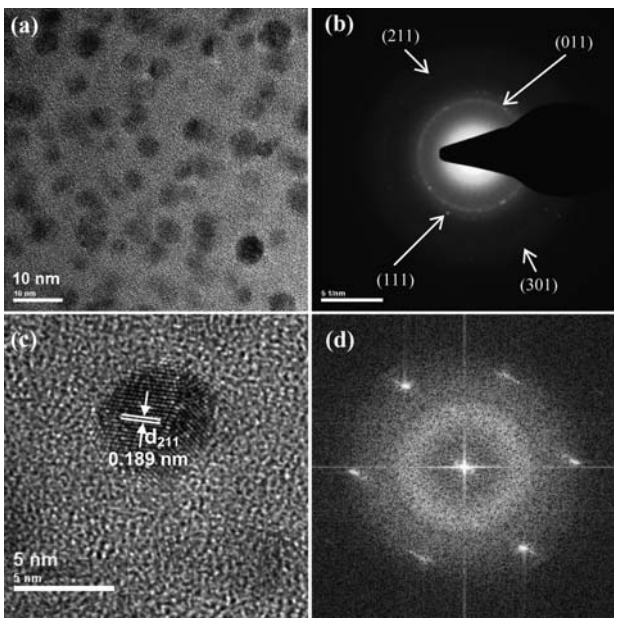

Fig. 10 (a) TEM image of orthorhombic CoP nanoparticles, (b) selected area electron diffraction (SAED) pattern, (c) HRTEM image, and (d) FFT of the HRTEM image; all images obtained from $[Co(Se_2P^tBu_2)_2]$ precursor in TOP/HDA at 300 °C for 150 min.

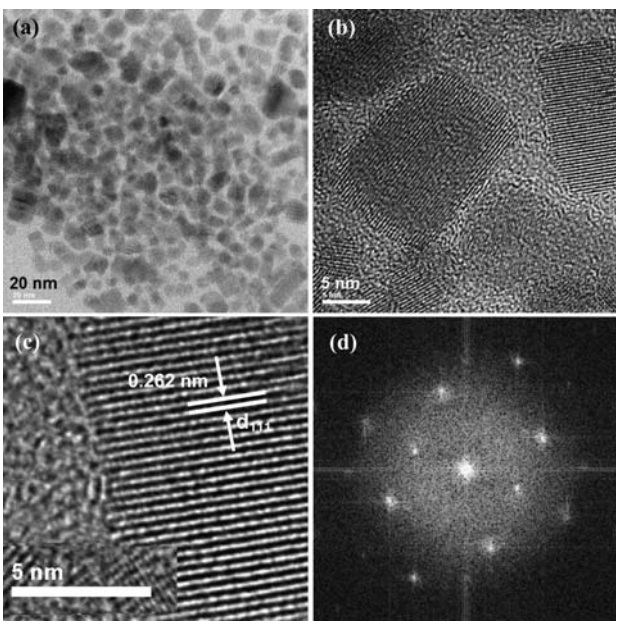

Fig. 11 (a) TEM image of orthorhombic $CoSe_2$ nanoparticles, (b) and (c) HRTEM images, (d) FFT of the HRTEM image; all images obtained from $[Co(Se_2P^tPr_2)_2]$ precursor in HDA at 320 °C for 120 min.

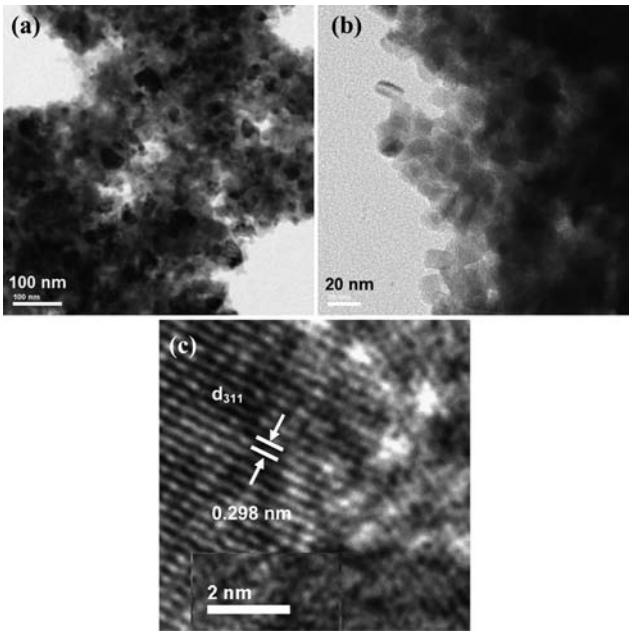

Fig. 12 (a) TEM image of aggregates of cubic Co_9S_8 nanoparticles, (b) Co_9S_8 nanoparticles with cuboid shape, and (c) HRTEM image; all images obtained from $[Co(S_2P^tBu_2)_2]$ precursor in HDA.

Conclusion

The dialkyldiselenophosphinatocobalt(II), $[Co(Se_2PR_2)]$ (R = ^{i}Pr, Ph and ^{t}Bu), and di-*t*-butyldithiophosphinatocobalt(II), $[Co(S_2P^tBu_2)_2]$, complexes have been proved to be the effective precursors for the preparation of cobalt phosphide, cobalt selenide or cobalt sulfide nanoparticles by changing the capping agent or deposition conditions. The capping agents, reaction times and reaction temperatures play important roles in chemical compositions as well as the morphology of the nanoparticles formed.

Acknowledgements

We thank the Royal Thai Government for funding. POB wrote this paper whilst a visiting fellow at Magdalen College, Oxford. He would like to thank the College for the Fellowship and the President and Fellows for being gracious hosts.

Notes and references

1 C. Stinner, R. Prins and T. Weber, *J. Catal.*, 2001, **202**, 187.
2 S. T. Oyama, T. Gott, H. Zhao and Y. K. Lee, *Catal. Today*, 2009, **143**, 94.
3 C. A. McAuliffe and W. Levason, *Phosphine, Arsine and Stibine Complexes of Transition Elements*, Elsevier, Amsterdam, 1979.
4 A. Panneerselvam, C. Q. Nguyen, J. Waters, M. A. Malik, P. O'Brien, J. Raftery and M. Helliwell, *Dalton Trans.*, 2008, 4499.
5 A. L. Hector and I. P. Parkin, *J. Mater. Chem.*, 1994, **4**, 279.
6 S. L. Brock, S. C. Perera and K. L. Stamm, *Chem.–Eur. J.*, 2004, **10**, 3364.
7 H. Hou, Q. Peng, S. Zhang, Q. Guo and Y. Xie, *Eur. J. Inorg. Chem.*, 2005, 2625.
8 H. Hou, Q. Yang, C. Tan, G. Ji, B. Gu and Y. Xie, *Chem. Lett.*, 2004, **33**, 1272.
9 C. M. Lukehart and S. B. Milne, *Chem. Mater.*, 1998, **10**, 903.
10 H. Wang, Y. Shu, A. Wang, J. Wang, M. Zheng, X. Wang and T. Zhang, *Carbon*, 2008, **46**, 2076.
11 Z. Zhang, J. Yang, Y. Nuli, B. Wang and J. Xu, *Solid State Ionics*, 2005, **176**, 693.
12 X. F. Qian, Y. Xie, Y. T. Qian, X. M. Zhang, W. Z. Wang and L. Yang, *Mater. Sci. Eng., B*, 1997, **49**, 135.
13 Y. Ni, J. Li, L. Zhang, S. Yang and X. Wei, *Mater. Res. Bull.*, 2009, **44**, 1166.
14 Y. Xie, H. L. Su, X. F. Qian, X. M. Liu and Y. T. Qian, *J. Solid State Chem.*, 2000, **149**, 88.
15 Y. Li, M. A. Malik and P. O'Brien, *J. Am. Chem. Soc.*, 2005, **127**, 16020.
16 J. Park, B. Koo, K. Y. Yoon, Y. Hwang, M. Kang, J. G. Park and T. Hyeon, *J. Am. Chem. Soc.*, 2005, **127**, 8433.
17 J. Yang, G. H. Cheng, J. H. Zeng, S. H. Yu, X. M. Liu and Y. T. Qian, *Chem. Mater.*, 2001, **13**, 848.
18 M. R. Gao, W. T. Yao, H. B. Yao and S. H. Yu, *J. Am. Chem. Soc.*, 2009, **131**, 7486.
19 C. E. M. Campos, J. C. de Lima, T. A. Grandi, K. D. Machado and P. S. Pizani, *Physica B (Amsterdam)*, 2002, **324**, 409.
20 Q. Lu, J. Hu, K. Tang, B. Deng, Y. Qian, G. Zhou and X. Liu, *Mater. Chem. Phys.*, 2001, **69**, 278.
21 W. Zhang, Z. Yang, J. Liu, Z. Hui, W. Yu, Y. Qian, G. Zhou and L. Yang, *Mater. Res. Bull.*, 2000, **35**, 2403.
22 A. Wold and K. Dwight, *J. Solid State Chem.*, 1992, **96**, 53.
23 D. M. Pasquariello, R. Kershaw, J. D. Passaretti, K. Dwight and A. Wold, *Inorg. Chem.*, 1984, **23**, 872.
24 B. Morris, V. Johnson and A. Wold, *J. Phys. Chem. Solids*, 1967, **28**, 1565.
25 L. F. Schneemeyer and M. J. Sienko, *Inorg. Chem.*, 1980, **19**, 789.
26 P. Barret, J. C. Colson and D. Delafosse, *C. R. Acad. Sci., Ser. IIc: Chim.*, 1966, **262**, 83.
27 C. Wang, X. M. Zhang, X. F. Qian, Y. Xie and Y. T. Qian, *J. Phys. Chem. Solids*, 1999, **60**, 2005.
28 Y. Zhang, F. Guo, S. Wan, W. Zheng and Y. Peng, *Bull. Chem. Soc. Jpn.*, 2005, **78**, 277.
29 F. Srouji, M. Afzaal, J. Waters and P. O'Brien, *Chem. Vap. Deposition*, 2005, **11**, 91.
30 A. Panneerselvam, M. A. Malik, M. Afzaal, P. O'Brien and M. Helliwell, *J. Am. Chem. Soc.*, 2008, **130**, 2420.
31 A. Panneerselvam, C. Q. Nguyen, M. A. Malik, P. O'Brien and J. Raftery, *J. Mater. Chem.*, 2009, **19**, 419.
32 F. S. Tihay, P. Braunstein, C. Estournès, J. L. Guille, B. Lebeau, J. L. Paillaud, M. Richard-Plouet and J. Rosé, *Chem. Mater.*, 2003, **15**, 57.
33 X. Song and M. Bochmann, *J. Chem. Soc., Dalton Trans.*, 1997, 2689.
34 W. Maneeprakorn, C. Q. Nguyen, M. A. Malik, P. O'Brien and J. Raftery, *Dalton Trans.*, 2009, 2103.
35 C. Q. Nguyen, A. Adeogun, M. Afzaal, M. A. Malik and P. O'Brien, *Chem. Commun.*, 2006, 2182.
36 T. Trindade and P. O'Brien, *Adv. Mater.*, 1996, **8**, 161.
37 S. C. Perera, G. Tsoi, L. E. Wenger and S. L. Brock, *J. Am. Chem. Soc.*, 2003, **125**, 13960.
38 A. E. Henkes and R. E. Schaak, *Chem. Mater.*, 2007, **19**, 4234.
39 Z. Yang and K. J. Klabunde, *J. Organomet. Chem.*, 2009, **694**, 1016.
40 R. K. Chiang and R. T. Chiang, *Inorg. Chem.*, 2007, **46**, 369.
41 W. Fan, R. A. Schoonheydt and B. M. Weckhuysen, *Phys. Chem. Chem. Phys.*, 2001, **3**, 3240.
42 B. M. Weckhuysen, R. R. Rao, J. A. Martens and R. A. Schoonheydt, *Eur. J. Inorg. Chem.*, 1999, 565.
43 J. Ackermann and A. Wold, *J. Phys. Chem. Solids*, 1977, **38**, 1013.
44 M. Sharon and G. Tamizhmani, *J. Mater. Sci.*, 1986, **21**, 2193.
45 N. F. Mott and E. A. Davis, *Electronic Processes in Non-Crystalline Materials*, Clarendon Press, Oxford, England, 1971.